IOP Conf. Series: Journal of Physics: Conf. Series **1037** (2018) 072054 doi:10.1088/1742-6596/1037/7/072054

Enrichment methods for inflow turbulence generation in the atmospheric boundary layer

E W Quon[1], A S Ghate[2], and S K Lele[3]

[1] National Wind Technology Center, National Renewable Energy Laboratory, Golden, CO 80401, USA
[2] Department of Aeronautics and Astronautics, Stanford University, Stanford, CA 94305, USA
[3] Department of Aeronautics and Astronautics and Department of Mechanical Engineering, Stanford University, Stanford, CA 94305, USA

E-mail: eliot.quon@nrel.gov

Abstract. We investigate the feasibility of introducing synthetic turbulence into finite-domain large-eddy simulations (LES) of the wind plant operating environment. This effort is motivated by the need for a robust mesoscale-to-microscale coupling strategy in which a microscale (wind plant) simulation is driven by mesoscale data without any resolved microscale turbulence. A neutrally stratified atmospheric boundary layer was simulated in an LES with 10-m grid spacing. We show how such a fully developed turbulence field may be reproduced with spectral enrichment starting from an under-resolved coarse LES field (with 20-m and 40-m grid spacing). The velocity spectra of the under-resolved fields are enriched by superimposing a fluctuating velocity field calculated by two turbulence simulators: TurbSim and Gabor Kinematic Simulation. Both forms of enrichment accurately simulated the autospectra of all three velocity components at high wavenumbers, with agreement between the enriched fields and the full-resolution LES observed at 400 m from the inflow boundary. In contrast, the spectra of the unenriched fields reached the same fully developed state at four times the downstream distance.

1. Introduction

High-fidelity wind plant simulation requires appropriate modeling of the fluid dynamics within the atmospheric boundary layer (ABL) across a wide range of scales. These scales include meteorological and environmental drivers at the mesoscale and a fully developed turbulence cascade at the microscale. To accurately predict the turbulent flow that impacts wind turbine performance, loads, and reliability, one must assess mesoscale effects including diurnal variation in radiative forcing, large-scale advection of heat and momentum, frontal passages, and complex terrain [6]. Incorporating these effects into a microscale large-eddy simulation (LES) requires downscaling from mesoscale data—either from simulation or measurements. Since the microscale LES is initialized with only large-scale features, significant spin-up time and upwind transition distance (also known as fetch) are required to fully develop the turbulence spectrum. Fetches on the order of 10 km or more have been observed in LES of the developing ABL [13, 14], and within this transition region, the simulated flow may not represent a realistic wind turbine operating environment. This fetch length varies depending on environmental conditions and can be comparable to the extent of a modern wind plant, necessitating significantly larger computational domains.

A number of different approaches may be applied to facilitate the transition to a turbulent field. Typical microscale LES will employ either a recycling method [10, 16], periodic precursor simulation [2, 16] or fringe region method [15]. These approaches are not necessarily tractable for general mesoscale-to-microscale coupling problems of interest due to auxiliary domain requirements and the associated computational cost of resolving the upwind fetch. For example, modeling wind plant inflow in complex terrain using a horizontally periodic precursor approach imposes the additional requirement that the terrain on corresponding mapped boundaries has a similar elevation. Typically, this would require extending the computational domain to include a buffer region and applying terrain smoothing [1].

As an alternative, the transition to fully resolved turbulence in the LES can be accelerated on a finite domain by superposing physically consistent perturbations to the downscaled mesoscale data. These data are analogous to unsteady Reynolds-Averaged Navier-Stokes (RANS) solution fields that do not include any resolved turbulence. Velocity perturbations [13] and potential temperature perturbations [14] can both help to initiate turbulent momentum and scalar transport, respectively. Perturbations add variance to the otherwise smooth inflow and enrich the spectra of the inflow by adding energy in the high-wavenumber range. This promotes development of turbulence throughout the range of LES-resolved microscales, thereby reducing upwind fetch and alleviating the computational burden. However, determination of appropriate perturbations is in itself a non-trivial task, and it can depend on *a priori* knowledge of flow characteristics including turbulence statistics, correlation functions, and integral length scales [11, 9, 18]. For realistic wind plant inflows, the perturbation strategy should be applicable for a variety of atmospheric stability states, which adds dependence on additional wall-modeling parameters including surface heat flux and roughness. Moreover, understanding of the limits of applicability for the different models is critical so that spurious features are not resolved within the *terra incognita* [17].

Given these unknowns, the present work focuses on enriching the velocity spectra using two different approaches. The first approach utilizes TurbSim, a stochastic turbulence generator that is a key component of the Fatigue, Aerodynamics, Structures, and Turbulence (FAST) wind turbine engineering model. TurbSim produces a turbulent time series of flow through a rotor plane based on an empirical spectral model for each velocity component and an empirical spatial coherence model [9]. Inputs are typically dictated by International Electrotechnical Commission (IEC) standards [7]. While TurbSim generates the correct inertial-range scaling for the turbulence autospectra, it lacks any information regarding cross-correlations when applying the standard IEC models.

A second and more physically rigorous approach is to enrich the spectral content of an inflow with a kinematic simulation (KS) using discrete Gabor modes [5]. This formulation uses Mann's [11] eddy-lifetime hypothesis together with Rapid Distortion Theory (RDT) to initialize log-spaced Gabor modes, in contrast to linearly spaced Fourier modes for Mann's original model. The use of non-uniform fast Fourier transforms allows for a fast inversion of the Gabor transform and for a substantially compressed representation of small-scale turbulence in terms of the spatially localized Gabor modes. The localized nature of these discrete modes allows for straightforward incorporation of non-stationary mesoscale forcings, Coriolis effects, stratification, and kinematic blocking produced by the terrain.

2. Methods

Our current study focuses on neutral atmospheric conditions with a prescribed 8 m/s wind speed at a nominal hub height of 90 m. Idealized stationary conditions have been considered to focus on the inhomogeneity of the flow associated with transition to fully developed turbulence. The LES is carried out using the Simulator fOr Wind Farm Applications (SOWFA) [3] on a 6 km x 3 km x 1 km domain (in the streamwise, lateral, and vertical directions, respectively). The solution is

initialized with a capping inversion in which the temperature increases linearly from 300 to 305 K between 700 and 800 m above the ground; above this strong inversion layer, the temperature continues to increase linearly at 3 K/km. A background pressure gradient is represented by a momentum source term, updated at each time step to drive the planar-averaged velocity to 8 m/s at hub height. An aerodynamic roughness height of 0.15 m was specified, resulting in a shear exponent of 0.21 with 11% turbulence intensity at hub height. Sub-grid-scale (SGS) modeling was provided by Deardorff's one-equation eddy viscosity model [4]. For simplicity, the Coriolis force has been set to zero.

To establish a reference solution, we perform an initial precursor calculation on a laterally periodic domain with a uniform grid spacing of $\Delta s = 10$ m and time-step size of $\Delta t = 0.5$ s. The mean values and turbulence statistics from this precursor are the baseline for this study. While a standard wind plant LES would directly sample time-varying inflow planes from this fully resolved turbulence simulation, we investigate simulation conditions in which a precursor is not viable and it is necessary to develop turbulence on a finite domain with inflow-outflow boundaries. To study the effectiveness of the spectral enrichment, we reduce the amount of resolved inflow turbulence by running additional precursors with coarser grid spacings (20 m and 40 m) and larger corresponding time steps (1.0 s and 2.0 s). The resulting fields are mapped to an inflow plane with 10-m resolution, and the following analysis will compare the fully resolved, periodic *baseline* simulation to the following finite-domain simulations:

(i) *Control*: Flow is under-resolved, with no spectral enrichment applied;

(ii) *TurbSim*: Velocity spectra are enriched according to case-specific physical and general empirical parameters; and

(iii) *Gabor KS*: Velocity spectra are enriched over a specified wavenumber range, according to case-specific physical parameters (summarized in Table 1).

The under-resolved precursor velocity fields are enriched by superimposing the fluctuating velocity field calculated by Gabor KS or TurbSim. To prevent double counting of sub-grid kinetic energy, the TKE from the coarse-grid precursors was set to zero. All of the inflow-outflow simulations use a grid identical to the 10-m precursor and retain the same conditions on all boundaries except the streamwise boundaries. Instead of being periodic, the inlet and outlet have time-varying Dirichlet and zero-gradient conditions, respectively. The 10-m finite-domain solution is initialized from the coarse-grid solution.

TurbSim enrichment depends on specified spectral and coherence models. The IEC Kaimal model, suitable for neutral stratification, was applied with the default parameters from the IEC 61400-1 standard. Parameters include the integral scale, a turbulence scale parameter, and the velocity standard deviation [7]. Spatial coherence was enforced in the u-component of velocity alone, dictated by standard IEC coherence decay and length-scale parameters [8]. Time-varying inflow planes were simulated for 10 minutes, a typical turbine aeroelastic simulation length. At each point on the inflow plane, the time series is generated by an inverse Fourier transform and the fluctuations repeat at 10-minute intervals. While the velocity fields synthesized by FAST have excellent two-point autocorrelations, they are generally not divergence free.

The Gabor KS approach computes small-scale structures that provide a consistent spectral extrapolation to larger scales that can be resolved by LES on much coarser numerical meshes. This is accomplished by compressing the flow-field modes into spatially localized wavepackets, requiring only 64^2 modes to represent over 10 million spatial degrees of freedom in the current case. The KS solves the simplified Gabor-transformed Navier-Stokes equations, which are a set of ordinary differential equations in time [5]. Local anisotropy in the enrichment field is parameterized in terms of two constants: a pre-distortion integral length scale of isotropic turbulence, L_{iso}; and a shear constant to scale the eddy lifetime, c_τ. The Gabor KS input parameters in Table 1 were tuned to match the total Reynolds stress at a reference location

of $z = 10$ m. As such, we will limit the analysis of the results to $z = 10$ m in the present work. While these constants can in principle be computed numerically, it assumes that the coarser simulations can accurately predict the mean flow profile and the total (sum of resolved and modeled) shear stress. However, as seen in Figure 1, the simulations at the two coarser resolutions deviate substantially from the fine-resolution simulation, even in terms of single-point first and second moments. This will be further discussed in Section 3.1.

Table 1: Gabor KS parameters

		$\Delta s = 20$ m	$\Delta s = 40$ m
wavenumber range	[1/m]	[0.05, 0.2]	[0.025, 0.2]
length scale, L_{iso}	[m]	98.5	25.0
shearing parameter, c_τ	[-]	2.41	3.50
reference $\langle u'w' \rangle$	[m^2 s^{-2}]	-0.045	-0.174
reference dU/dz	[s^{-1}]	0.106	0.0529

At this stage, we can identify two distinct components of the enrichment problem:

(i) An adequate representation of large-scale flow features in the coarser simulations is needed. This is a nuanced problem dealing with the interplay between SGS closure, numerics, and wall modeling. While this is a key element of the problem, it is beyond the scope of the present work.

(ii) Given an accurate representation of the larger scales, a reliable approach to generate the smaller scales of turbulence is needed. These synthetic fields must be consistent with the large scales resolved by the coarser LES.

In this paper, we will tackle the latter problem, acknowledging that the larger scales created by the coarser LES have substantial differences from what one would expect from a finer-resolution LES filtered down to the coarser mesh. Since the enrichment is intended to extrapolate the spectral content of the large scales, the finer enriched scales must depend on the distance from the ground. As a first step, however, we have assumed vertical homogeneity to provide consistency between TurbSim and Gabor KS. The enriched small scales are set to zero above a certain height ($z = 225$ m and $z = 625$ m for the $\Delta s = 20$ m and $\Delta s = 40$ m cases, respectively) at which the unresolved shear stress is deemed negligible. The cutoff is applied as a hyperbolic tangent function with a width of approximately 50 m, which is sufficiently large to avoid significant spurious divergence.

3. Results and Discussion

The results in this paper have been separated into three parts: an evaluation of the coarse-resolution, under-resolved control LES; analysis of single-point correlations in the control and enriched LES cases; and analysis of two-point correlations in the control and enriched LES cases.

3.1. Quality of the coarse-resolution LES

Statistics of the periodic precursor simulations are shown in Figure 1 for three different grid spacings: 10 m, 20 m, and 40 m. The computational cost of the calculations at 20-m and 40-m resolution is approximately 1/16 and 1/256 the cost of the baseline calculation. Therefore, the added cost to resolve the microscale fetch may be negligible. Note that the 40-m resolution case corresponds to only 25 uniformly spaced grid points used to discretize the entire vertical domain. As a result, the vertical profiles of the resolved flux Richardson number (defined in this case as $Ri_f = \frac{(g/T_0)\langle w\theta \rangle}{\langle uw \rangle dU/dz}$) show that the inversion layer at 40-m resolution is unable to

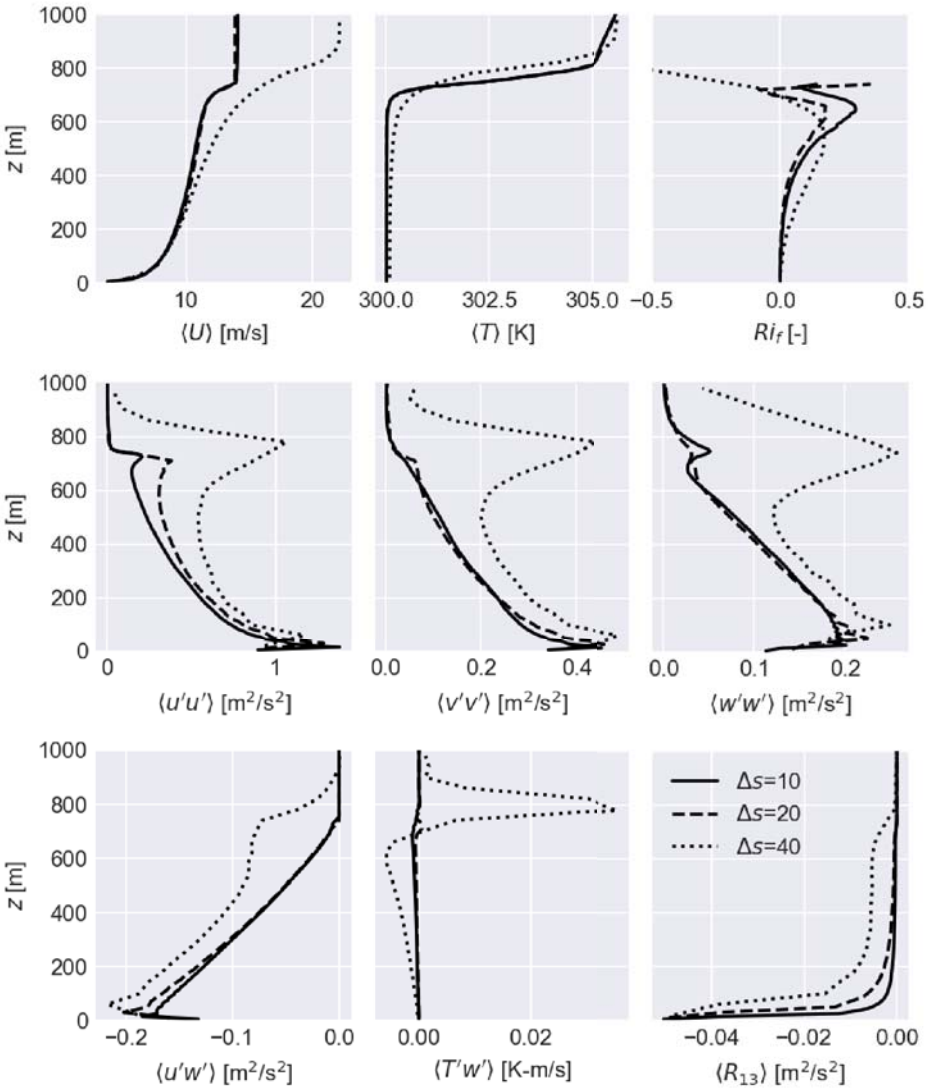

Figure 1: Planar-averaged (indicated by $\langle\cdot\rangle$) vertical profiles of wind speed (U), temperature (T), flux Richardson number (Ri_f), variances ($u'u'$, $v'v'$, $w'w'$), and resolved covariances ($u'w'$ and $T'w'$) and modeled shear stress (R_{13}) for different uniform precursor spatial resolutions.

cap the growth of the turbulent boundary layer since the LES filter scale is vastly larger than the expected Ozmidov scale. Moreover, the complex subfilter physics cannot be adequately modeled by the SGS model, and consequently, the mean flow properties through the bulk of the boundary layer are vastly overpredicted. A second-moment RANS closure approach [12], with finer vertical resolution and larger aspect-ratio grids, may be needed to capture mean turbulent boundary-layer properties at such coarse resolutions.

Figure 2 shows the time history of the horizontally averaged friction velocity, $u^\star$, for the inflow-outflow simulations that use inflow and initialize from the coarser resolution precursors. All the cases originating from the 20-m precursor converge rapidly, to within 2% of the reference precursor after about 140 s. The initial transients observed with 40-m grid spacing correspond to the readjustment of the large-scale and mean-flow features to the finer grid. After approximately 3000 s, the flow field has converged to the 10-m periodic precursor result.

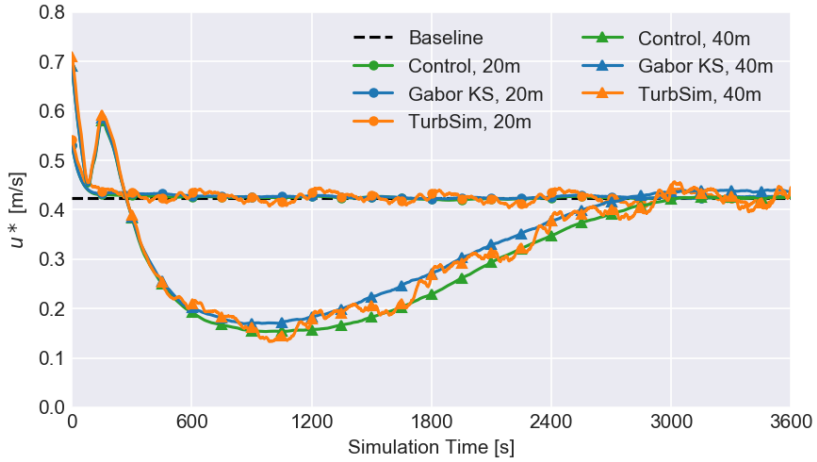

Figure 2: Time history of averaged friction velocity (u^*) for baseline, coarse-resolution-unenriched (control), and coarse-resolution-enriched (with Gabor KS or TurbSim) LES.

3.2. Single-point correlations as a function of distance from the inlet

Next, we evaluate the streamwise evolution of the pertinent single-point correlations as a function of downstream distance from the inlet, at a fixed elevation of 10 m (Figures 3–4). At 20-m grid spacing, both the enriched (unreported for clarity) and the control cases attain the baseline correlations very rapidly since the bulk of the large scales are accurately modeled in the corresponding precursor simulations. However, the 40-m results appear to require a substantial fetch (over 1 km) before the single-point correlations converge to the baseline result. While there is some evidence that the enrichment methods promote turbulence development, the flow field responds differently to the two perturbation methods and can result in a slight overshoot (v-velocity variance) or undershoot (u- and w-velocity variances, TKE). Therefore, it is not clear whether enrichment provides substantial improvement over the control cases when only single-point correlations are considered. The standard deviation in the single-point correlations of the baseline results, indicated by the shaded region most visible in the u-velocity variance and TKE, confirms that the difference in converged statistics between the reduced-resolution precursor and baseline is statistically significant. This can be attributed to the inadequacy of the coarse 40-m-resolution precursor in generating accurate large-scale turbulence structures. Hence, the downstream flow evolution is dominated by large-scale flow restructuring that occurs once the inflow enters the domain.

3.3. Two-point correlations as a function of distance from the inlet

Figure 5 shows the k_y spectra at $z = 10$ m as a function of downstream distance from the inlet. The spectra at $x = 100$ m suggest that both enrichment methods appear to extrapolate the low k spectrum from the coarse 40-m LES. However, it seems that the enrichment methods are unable to capture the k^{-1} production-range scaling evident in the baseline simulation; the enriched fields instead tend towards the inertial range $k^{-5/3}$ scaling. While this $-5/3$ scaling is explicitly specified in the TurbSim approach (within the Kaimal spectral model), it is not explicitly contained within the Gabor KS. This may therefore be a consequence of significant over-prediction of the integral length scale in the coarser simulations.

Furthermore, the E_{33} spectrum at $x = 100$ m (Figure 5g) suggests that the enriched Gabor KS fields have inaccurate anisotropy since the vertical fluctuations at scales up to $k_y \sim 0.1$ m^{-1} (i.e., length scales of about 60 m) are not sufficiently damped by the large mean shear. This

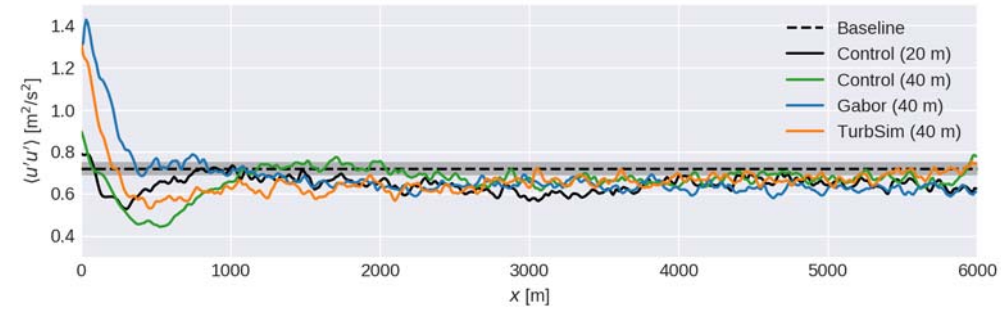

(a) u-velocity variance

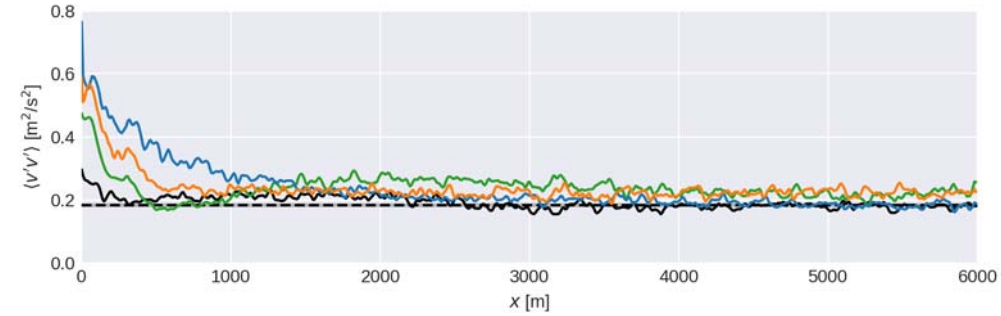

(b) v-velocity variance

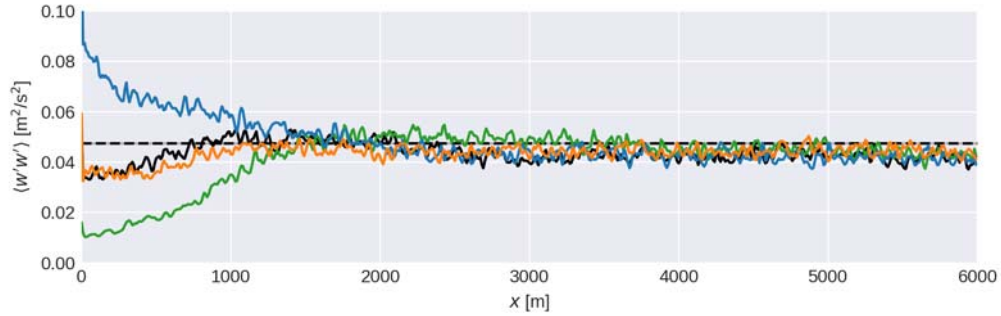

(c) w-velocity variance

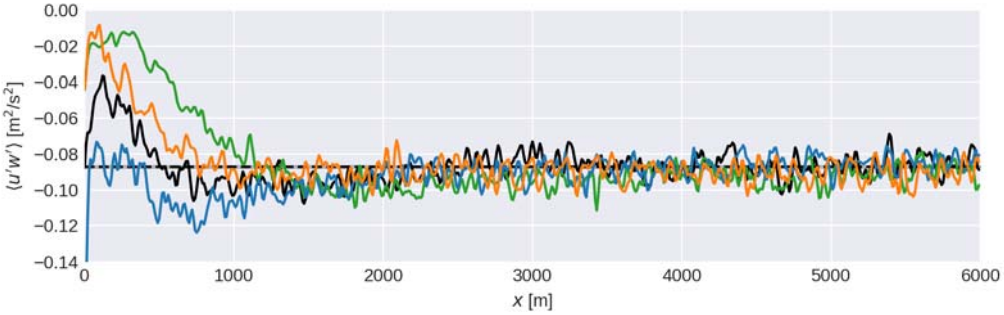

(d) u, w-velocity covariance

Figure 3: Evolution of variances at $z = 10$ m.

may be a consequence of overestimating the pre-distortion isotropic length scale, L_{iso}, which subsequently resulted in underestimation of the shearing coefficient, c_τ. This observation is consistent with the theme observed in the single-point correlations; the Gabor KS enrichment outperforms the control and TurbSim cases for $\langle u'u' \rangle$, but has slightly slower convergence in

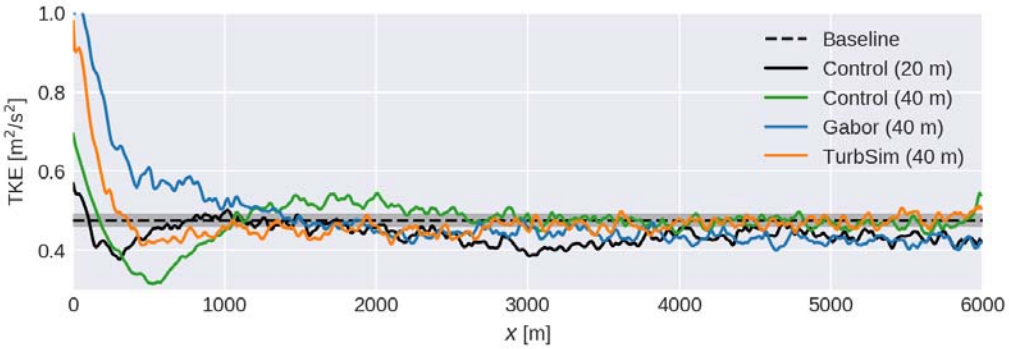

Figure 4: Evolution of turbulent kinetic energy (TKE) at $z = 10$ m.

$\langle v'v' \rangle$ and $\langle w'w' \rangle$. This aspect can be remedied by improving the estimates for L_{iso}.

We finally observe that both enrichment methods result in significant acceleration in the development of high-wavenumber (small-scale) features compared to the control case. At about 400-m downstream of the inlet, spectral characteristics from the enriched coarse-resolution simulations are comparable to the baseline full-resolution results. In contrast, agreement between the control and baseline simulations is not observed until about 1600 m downstream.

4. Conclusions

Our results have clearly demonstrated that spectral enhancement methods produce the correct spectra in the high-wavenumber range. In all three velocity components, the spectra for the enriched coarse-precursor inflow—with grid resolution reduced by a factor of four to 40 m—developed the same spectral characteristics as the full-resolution (10 m) precursor. This fully developed turbulent inflow was observed over a kilometer closer to the inlet than the unenriched control case. As seen from the evolution of one-point statistics, the applied perturbations persist through the interior of the computational domain and develop the same auto- and cross-correlations as the baseline precursor solution. This held true even for cases in which suboptimal spectral enrichment resulted in over-enrichment, due to the fact that turbulence development is dominated by the largest resolved scales in the LES. These results highlight two fundamental requirements for turbulent inflow generation: appropriate high-wavenumber enrichment and accurate low-wavenumber SGS modeling. While we have shown that high-wavenumber enrichment is successful, it is also apparent that the minimum time and fetch required for transition to fully developed turbulence are dictated by the accuracy of the SGS model.

The enrichment methods applied here may be further optimized. While the simplest implementation of the Gabor KS has been used in this study, effects such as kinematic blocking and vertical variation in correlations can be modeled using Gabor modes. This would also eliminate the need to scale the enriched velocity fluctuations to zero above a specified inversion height—a height that must be known *a priori*—since the Gabor-KS enrichment would naturally decay with increasing wall-normal distance. This is consistent with the fact that the integral length scale increases with wall-normal distance thus enabling the coarse LES to capture more of the energy in the flow. Furthermore, the Gabor formulation allows for slow changes to the geostrophic and mean flow as a function of time. Since the straining of small-scale turbulence by the mean flow and buoyancy (via the Boussinesq approximation) is represented in the governing equations, evolving boundary-layer stratification may also be modeled. The TurbSim simulations may also be further refined, either with a different spectral model or through optimization of the spectral-model and coherence-model parameters.

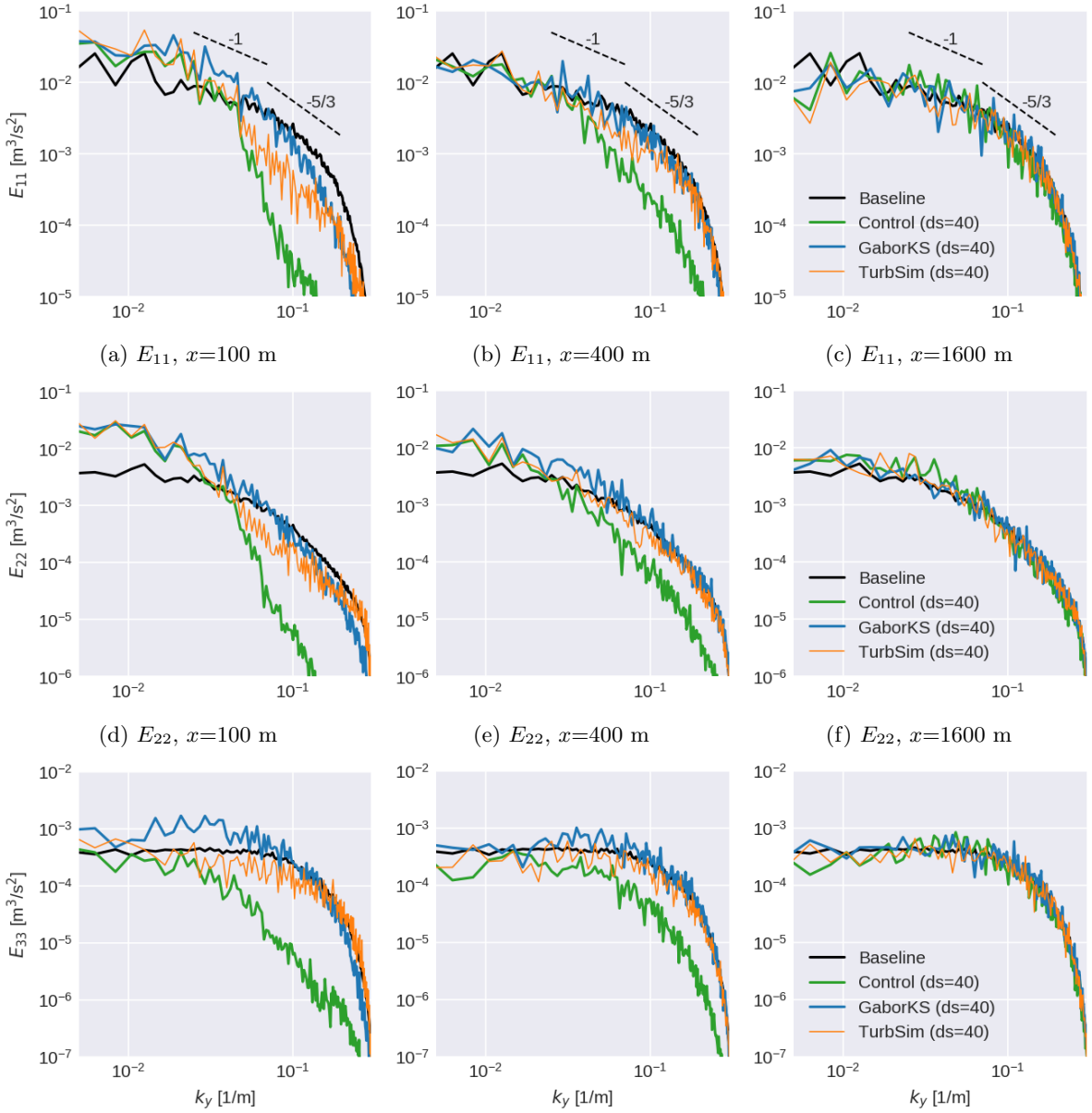

(a) E_{11}, x=100 m (b) E_{11}, x=400 m (c) E_{11}, x=1600 m

(d) E_{22}, x=100 m (e) E_{22}, x=400 m (f) E_{22}, x=1600 m

(g) E_{33}, x=100 m (h) E_{33}, x=400 m (i) E_{33}, x=1600 m

Figure 5: Streamwise evolution (from left to right) of u-, v-, and w-velocity autospectra (top, middle, and bottom rows) at $z = 10$ m.

The challenges that we encountered in this study are likely to be observed in practical applications of mesoscale-to-microscale-coupled LES on a finite domain. Such a simulation would likely include a reduced-resolution region to accommodate the development of turbulence with minimal added cost. The formation of the largest scales of turbulence would also be heavily dependent upon the SGS model behavior. One possibility for extending the enrichment methodology from the inertial subrange into the energy-containing scales is to couple the turbulence simulator to a reduced-order model that would encapsulate the larger-scale turbulence dynamics. A natural strategy for this modeling approach would be to perform a space-

time proper orthogonal decomposition or dynamic mode decomposition on high-resolution data filtered down to coarser grids. Overall, the enrichment strategies explored in this paper have the promise to be an essential part of any mesoscale-to-microscale coupling framework.

Acknowledgements

Aditya Ghate was funded via a seed grant provided by the Tomkat Center for Sustainable Energy at Stanford University. Many thanks go out to Matt Churchfield for his guidance and expertise.

The Alliance for Sustainable Energy, LLC (Alliance) is the manager and operator of the National Renewable Energy Laboratory (NREL). NREL is a national laboratory of the U.S. Department of Energy, Office of Energy Efficiency and Renewable Energy. This work was authored by the Alliance and supported by the U.S. Department of Energy under Contract No. DE-AC36-08GO28308. Funding was provided by the U.S. Department of Energy Office of Energy Efficiency and Renewable Energy. The views expressed in the article do not necessarily represent the views of the U.S. Department of Energy or the U.S. government. The U.S. government retains, and the publisher, by accepting the article for publication, acknowledges that the U.S. government retains a nonexclusive, paid-up, irrevocable, worldwide license to publish or reproduce the published form of this work, or allow others to do so, for U.S. government purposes.

References

[1] J Berg, N Troldborg, N N Sørensen, E G Patton, and P P Sullivan. Large-eddy simulation of turbine wake in complex terrain. *J. Phys. Conf. Ser.*, 854(012003):1–7, 2017.
[2] M J Churchfield, S Lee, J Michalakes, and P J Moriarty. A numerical study of the effects of atmospheric and wake turbulence on wind turbine dynamics. *J. Turbul.*, 13(14):1–32, 2012.
[3] M J Churchfield, S Lee, P J Moriarty, L A Martinez, S Leonardi, G Vijayakumar, and J G Brasseur. A Large-Eddy Simulation of Wind-Plant Aerodynamics. In *50th AIAA Aerospace Sciences Meeting*, 2012.
[4] J W Deardorff. Stratocumulus-capped mixed layers derived from a three-dimensional model. *Bound.-Layer Meteorol.*, 18:495–527, 1980.
[5] A S Ghate and S K Lele. Subfilter-scale enrichment of planetary boundary layer large eddy simulation using discrete Fourier–Gabor modes. *J. Fluid Mech*, 819:494–539, 2017.
[6] S E Haupt *et al.* Third-Year Report of the Atmosphere to Electrons Mesoscale-to-Microscale Coupling Project. Technical report, Pacific Northwest National Laboratory, 2017.
[7] IEC. Wind turbines – Part 1: Design requirements. Technical Report IEC 61400-1, Edition 3.1, International Electrotechnical Commission, Geneva, Switzerland, 2014.
[8] B J Jonkman and M L Buhl. TurbSim User's Guide. Technical Report NREL/TP-500-3979, National Renewable Energy Laboratory, 2006.
[9] N D Kelley. Turbulence-Turbine Interaction: The Basis for the Development of the TurbSim Stochastic Simulator. Technical Report NREL/TP-5000-52353, National Renewable Energy Laboratory, 2011.
[10] T S Lund, X Wu, and K D Squires. Generation of turbulent inflow data for spatially-developing boundary layer simulations. *J. Comput. Phys.*, 140(2):233–58, 1998.
[11] J Mann. The spatial structure of neutral atmospheric surface-layer turbulence. *J. Fluid Mech.*, 273:141–68, 1994.
[12] G L Mellor and T Yamada. Development of a turbulence closure model for geophysical fluid problems. *Rev. Geophys*, 20(4):851–75, 1982.
[13] J Mirocha, B Kosović, and G Kirkil. Resolved turbulence characteristics in large-eddy simulations nested within mesoscale simulations using the weather research and forecasting model. *Mon. Wea. Rev.*, 142(2):806–31, 2014.
[14] D Muñoz-Esparza, B Kosović, J van Beeck, and J Mirocha. A stochastic perturbation method to generate inflow turbulence in large-eddy simulation models: Application to neutrally stratified atmospheric boundary layers. *Phys. Fluids*, 27(3):035102, 2015.
[15] J Nordström, N Nordin, and D Henningson. The fringe region technique and the fourier method used in the direct numerical simulation of spatially evolving viscous flows. *SIAM J. Sci. Comput*, 20(4):1365–93, 1999.
[16] X Wu. Inflow turbulence generation methods. *Annu. Rev. Fluid Mech.*, 49(1):23–49, 2017.
[17] J C Wyngaard. Toward numerical modeling in the "terra incognita". *J Atmos. Sci.*, 61:1816–26, 2004.
[18] Z-T Xie and I P Castro. Efficient generation of inflow conditions for large eddy simulation of street-scale Flows. *Flow Turbul. Combust*, 81(3):449–70, 2008.